Hardness Analysis for Elastic-Plastic Layered Media

N. Ye, Graduate Student
K. Komvopoulos, Professor, Fellow ASME
Department of Mechanical Engineering
University of California
Berkeley, CA 94720

Abstract

An analysis of elastic-plastic layered media indented by a rigid sphere is developed based on finite element simulation results in order to determine the conditions for measuring the real material hardness. The critical interference distance, below which substrate effects are insignificantly small, is determined from the variation of the equivalent hardness with the interference distance. A relation between hardness, yield strength, and elastic modulus, derived from finite element indentation simulations of a homogeneous medium, is used in conjunction with a previously developed contact constitutive model, to determine the minimum interference distance, above which sufficient plasticity occurs in order to obtain the real material hardness. A new scheme of hardness measurement for layered media is presented and validated by finite element results for an elastic-perfectly plastic layered medium.

1. Introduction

Hardness is a property characterizing the resistance of a material to indentation and wear. In traditional indentation tests, the applied normal load is of the order of hundreds to thousands of Newtons and the diameter of the indentation is of the order of micrometers to millimeters. Recently, hardness testing has evolved from microhardness to nanohardness measurement, where residual impressions have diameters of the order of micrometers or even nanometers, measured with high-power microscopes or atomic force microscopes. This is a result of the increasing use of layered media in various engineering applications where surface durability is of critical importance. Micro- and nano-indentation testing for layered media is an effective method of extracting information about the mechanical properties of thin surface layers. As a consequence, a large number of theoretical and experimental indentation studies have been performed to elucidate the effect of the surface layer on the mechanical response of layered media.

Pharr (1998) reviewed and discussed techniques for measuring mechanical properties by ultra-low load indentation techniques. Emphasis was given on the measurement of the elastic modulus and hardness using sharp indenters. One of the most widely used methods is that of Oliver and Pharr (1992), which expands on ideas developed by Loubet et al. (1984) and Doerner and Nix (1986). In this method, hardness and elastic modulus can be determined from load and displacement sensing in indentation experiments. Lichinchi et al. (1998) used the finite element technique to study the stress-strain field in thin hard coatings subjected to nanoindentation loading. For titanium nitride coatings on high-speed steel, the substrate material was found to exhibit an effect on the hardness measurement for indentation depths greater than 15% of the film thickness. Pelletier et al. (2000) used the finite element method to analyze hardness measurement with a sharp pyramidal indenter, such as a Berkovich or Vickers indenter. The indenter tip radius was shown to exhibit a strong effect on the load-displacement response. A method was proposed to determine the tip radius of an equivalent conical indenter that was used in the finite element analysis as an approximation of the Berkovich indenter. Chen and Vlassak (2001) used the finite element method to investigate substrate and pileup effects on hardness and stiffness measurements of layered media. They defined a substrate effect factor and constructed a map that may be useful in the interpretation of indentation measurements when it is not possible to obtain sufficiently shallow indentations to avoid the influence of the substrate on the measurements. Martinez and Esteve (2001) studied nanoindentation of very hard and elastic thin layers, and reported that the hardness measured with a blunt indenter exhibited significant variation at small penetration depth.

The mechanical properties of a layered medium measured from indentation tests, such as hardness and elastic modulus, include the combined response of both the surface layer and the substrate materials. Bhattacharya and Nix (1988) studied the elastic and plastic deformation due to indentation of thin layers on relatively harder and softer substrates using the finite element method and derived semi-empirical relations for the hardness in terms of interference distance, layer thickness, and elastic-plastic material properties of the layer and the substrate. King (1987) analyzed the normal contact problem of a layered isotropic elastic half-space using basis function and singular integral equation technique, and modified the relation for the effective elastic modulus of a layered medium, originally proposed by Doerner and Nix (1986).

The previous studies enable us the determination of the layer hardness and elastic modulus from the equivalent hardness and elastic modulus of the layered medium when the substrate properties are known, although in the model of Bhattacharya and Nix (1988) a relation between the hardness and yield strength of layer is required. Despite valuable insight into indentation mechanics and hardness measurement of layered media, there are several important issues requiring further analysis in order to determine the conditions under which the real hardness can be obtained. For example, if substrate properties are unknown, under what conditions can the layer hardness be approximated by the equivalent hardness? Another important issue is the minimum interference distance for a valid hardness measurement. Hence, the main objective of this study is to provide an analysis that gives answers to the previous issues. The critical interference distance to avoid the substrate effect was derived using the model of Bhattacharya and Nix (1988). A contact constitutive model, presented in a previous study (Komvopoulos and Ye, 2001) was used in conjunction with experimental results from other studies to derive the minimum interference distance for measuring the real material hardness. A general relation between hardness, yield strength, and elastic modulus, obtained from a finite element model, was used together with the model of Bhattacharya and Nix (1988) to obtain a scheme of extracting layer material properties. Example calculations are given to illustrate the appropriateness and predictability of the presented analytical scheme for hardness measurement.

2. Finite Element Model

An axissymmetric finite element model was developed using the general-purpose finite element code ABAQUS to simulate indentation of a homogeneous or layered medium by a rigid sphere of radius R. Figure 1 shows the mesh of the finite element model, which consists of 218 eight-node isoparametric axissymmetric elements with a total of 677 nodes. The normalized dimensions of the mesh are $x/R = z/R = 8$. The nodes of the bottom boundary of the mesh were constrained in the z-direction and the nodes of the symmetry axis ($x = 0$) were constrained against the x-direction. A series of homogeneous half-spaces with different effective elastic modulus-to-yield strength ratio, E^*/s_Y ($E^* = \left[\left(1-n_1^{\,2}\right)/E_1 + \left(1-n_2^{\,2}\right)/E_2\right]^{-1}$, where n_1, n_2, and E_1, E_2 are the Poisson's ratios and elastic moduli of the half-space and rigid sphere) were analyzed. The materials were assumed to exhibit elastic-perfectly plastic behavior. The layer and substrate material properties used in the finite element model are listed in Table 1. Contact between the rigid sphere and the half-space medium was modeled with special contact elements, and the contact interface was assumed to be frictionless. Typically, an indentation simulation was completed in 5 time steps, each consisting of 100-500 increments. The computation time on an Intel Pentium III 550 workstation was between 2400 and 3600 CPU seconds.

3. Hardness Analysis

A theoretical treatment of the hardness of layered media is introduced in this section. The analysis yields the critical interference distance, above which the effect of the substrate material on the equivalent hardness of the layered medium is significant, and the minimum interference distance, below which the occurrence of insufficient plastic deformation in the layer prevents the direct measurement of material hardness.

3.1 Critical Interference Distance to Avoid the Substrate Effect

If the mechanical properties of the substrate are unknown, the layer hardness can be approximated by the hardness measured from an indentation test performed on the layered medium, provided the indentation depth (interference distance) is sufficiently small to avoid the effect of the deformation of the substrate. The indentation hardness relations of Bhattacharya and Nix (1988) for relatively hard and soft surface layers can be used to determine the critical interference distance for the substrate effect to be insignificant.

For a layer harder than the substrate, the equivalent hardness, H_e, is given by

(Bhattacharya and Nix, 1988)

$$\frac{H_e}{H_l} = \frac{H_s}{H_l} + \left(1 - \frac{H_s}{H_l}\right) \exp\left[- \frac{(H_l / s_l)}{(H_s / s_s)} \left(\frac{d}{h}\right) \left(\frac{E_s}{E_l}\right)^{1/2} \right], \qquad (1)$$

where H is the hardness, h is the layer thickness, E is the elastic modulus, s is the yield strength, d is the interference distance between the indenter and the surface of the deformable medium, and subscripts l and s denote the layer and substrate material properties, respectively. Equation (1) can be rewritten as,

$$H_e = H_l e^{-b} + H_s (1 - e^{-b}), \qquad (2)$$

where

$$b \equiv \frac{(H_l / s_l)}{(H_s / s_s)} \left(\frac{d}{h}\right) \left(\frac{E_s}{E_l}\right)^{1/2} . \qquad (3)$$

For the equivalent hardness to be close to the layer hardness, the contribution of the first term of Eq. (2) must be appreciably greater than that of the second term. Hence,

$$\frac{H_s (1 - e^{-b})}{H_l e^{-b}} \leq x , \qquad (4)$$

where x is a tolerance parameter less than 1 (e.g., x = 10%) indicating that the contribution of the substrate material deformation to the hardness measurement is negligibly small. Then, the critical interference distance to avoid the substrate effect can be written as

$$\frac{d}{h} \leq \ln(x \frac{H_l}{H_s} + 1) \left(\frac{E_l}{E_s}\right)^{1/2} \frac{(H_s / s_s)}{(H_l / s_l)} \qquad (5)$$

According to Eq. (5), the critical interference distance is a function of the tolerance parameter, elastic-plastic material properties of the layer and the substrate media, and layer thickness. Since for a layer harder than the substrate,

$$\left(\frac{E_l}{E_s}\right)^{1/2}\frac{(H_s / s_s)}{(H_l / s_l)} \geq 1, \tag{6}$$

Eq. (5) is satisfied if $d / h \leq \ln(x+1)$. For $x << 1$, $\ln(x+1) \approx x$, and Eq. (5) can be approximated as

$$\frac{d}{h} \leq x\,. \tag{7}$$

Thus, according to this empirical relation (Eq. (7)) the critical interference distance depends on the selected tolerance constant and hard layer thickness.

For a layer softer than the substrate, the effect of the substrate material deformation on the equivalent hardness can be determined from relation (Bhattacharya and Nix, 1988),

$$\frac{H_e}{H_l} = \frac{H_s}{H_l} + \left(1 - \frac{H_s}{H_l}\right)\exp\left[-\frac{(s_l / E_l)}{(s_s / E_s)}\left(\frac{d}{h}\right)^2\right]. \tag{8}$$

Thus, the critical interference distance is given by

$$\left(\frac{d}{h}\right)^2 \leq \ln(x\ \frac{H_l}{H_s} + 1)\frac{(s_s / E_s)}{(s_l / E_l)} \tag{9}$$

For a layer softer than the substrate,

$$\frac{(s_s / E_s)}{(s_l / E_l)} \leq 1, \tag{10}$$

and $x\ \frac{H_l}{H_s} << 1$, Eq. (9) can be rewritten as,

$$\frac{d}{h} \leq \sqrt{x\ \left(\frac{H_l}{H_s}\right)} \tag{11}$$

Although the critical interference distance can be determined from Eq. (5) (or Eq. (9)), the minimum interference distance to obtain the layer hardness cannot be obtained from this equation. According to Eq. (1) (or Eq. (8)), when the interference distance approaches zero, the measured hardness approaches the layer hardness. Since this is true only for a pyramidal indenter with infinitely sharp tip (i.e., zero tip radius of curvature), Eq. (1) (or Eq. (8)) cannot be used for shallow indentations, where the assumption of infinitely sharp indenter tip is not valid. Hence, it is necessary to obtain an analysis of material indentation by a finite tip radius indenter.

3.2 Relation Between Hardness, Yield Strength, and Elastic Modulus

For a spherical indenter and relatively small interference distance, the resulting small plastic zone may yield a mean contact pressure that is not representative of the layer hardness. This is demonstrated by finite element simulation results shown in Figs. 2-4 for a homogeneous medium with effective elastic modulus-to-yield strength ratio E^*/s_Y = 10, 33, 100, and 200 indented by a rigid sphere. Figure 2 shows the dependence of the mean contact pressure, p_m, on representative strain $E^* d / s_Y r'$, where s_Y is the yield strength and r' is the radius of the truncated contact area. For all material properties, the mean contact pressure increases with representative strain to a peak value and then decreases, in agreement with the findings of Mesarovic and Fleck (1999), who observed a decrease of the mean contact pressure after rising to a value of about 3 times the yield strength for $E^*/s_Y \geq 250$. Figure 2 shows that the peak value of the normalized mean contact pressure depends on E^*/s_Y. This is consistent with the observation of Marsh (1964), who performed a series of indentation tests with various materials.

Figures 3 and 4 show the evolution of plasticity in the subsurface of homogeneous elastic-perfectly plastic half-space media with E^*/s_Y = 10 and 100, respectively. There are some similarities between the plastic zones in the two half-spaces. The general trend is for the plastic zone to expand radially as the indenter penetrates deeper in the medium (Figs. 3(a), 3(b), 4(a), and 4(b)). The plastic zone is initially contained in the subsurface surrounded by elastic material. Deeper indentations cause spreading of the plastic zone to the surface (Figs. 3(c), 3(d), 4(c), and 4(d)). However, a comparison of Figs. 3(a) and 4(d) shows that for a similar interference distance, the material with the higher E^*/s_Y value yields a much larger plastic zone. Moreover, the plastic zone of the material with lower E^*/s_Y occurs always below the contact region, while the plastic zone of the material with higher E^*/s_Y spreads outside of the contact region after reaching the surface (Fig. 4(d)). The representative strain corresponding to the plastic zones shown in Figs. 3(d) and 4(d) is associated with the maximum value of the mean contact pressure. The representative strain and mean contact pressure for each plastic zone shown in Figs. 3 and 4 are given in Table 2. The maximum value of p_m/s_Y for E^*/s_Y = 10 and 100 is equal to 1.71 and 2.58, respectively.

Since the mean contact pressure depends on the representative strain (or interference distance), it is not straightforward to determine which is the interference distance (or strain) that yields the material hardness. A unique hardness value can be determined if the peak value of the mean contact pressure is set equal to the material hardness. This is consistent with the hardness definition of ductile materials, such as metals with typically $E^*/s_Y > 200$, for which full plasticity is more easily achieved, where the maximum contact pressure (hardness) is equal to ~$3s_Y$. However, as shown in Fig. 2, the peak contact pressure-to-yield strength ratio depends on the elastic-plastic material properties.

Before introducing the minimum interference distance for hardness measurement, it is instructive to examine the relation between hardness, yield strength, and elastic modulus of elastic-plastic homogeneous materials. Finite element results for the material hardness, *H* (assumed equal to the peak value of the mean contact pressure) are plotted in Fig. 5 and compared with experimental results obtained by Marsh (1964). The difference between simulation and experimental results is attributed to the Vickers indenter used in the experimental study and the constitutive relation adopted in the finite element simulations that may not be appropriate for the experimental materials. Since shallow indentations are required for the determination of the minimum interference distance to obtain an accurate measurement of the layer hardness, a spherical indenter approximates more closely those used in this type of indentation tests. According to the best-fit line of the numerical data (with a correlation coefficient of 0.99), the material hardness is given by

$$\frac{H}{s_Y} = 0.90 + 0.37 \ln\left(\frac{E^*}{s_Y}\right), \qquad (10 \le E^*/s_Y \le 200)\,. \qquad (12)$$

As pointed out previously, for very thin layers, the interference distance (i.e., indention depth) must be sufficiently small in order to avoid the effect of the substrate material properties on the hardness measurement. However, if the indentation is too shallow, plastic deformation in the layer may be limited and the resulting mean contact pressure may not be representative of the layer hardness. Although mean contact pressure values can be obtained at any given indentation depth from the indentation load-depth curve, the mean contact pressure will not be equal to the layer hardness if the interference distance is not sufficient for the plastic zone in the layer to be fully developed. Thus, if the minimum interference distance is not reached, the layer hardness will be underestimated.

3.3 Minimum Interference Distance for Layer Hardness Measurement

A relation for the minimum interference distance required for the mean contact pressure to reach a value equal to the material hardness can be derived using Eq. (12) and the contact constitutive model of the normalized mean contact pressure and the representative strain for a spherical indenter in normal contact with a homogeneous medium derived in a previous study (Komvopoulos and Ye, 2001). According to this analysis, elastic, elastic-plastic, and fully-plastic deformation regimes may occur. Clearly, interference distances corresponding to the elastic regime cannot be used to determine the hardness because deformation in this regime is purely elastic. Furthermore, in the fully-plastic regime the mean contact pressure is invariant. However, in view of the continuous transition from the elastic-plastic to the fully-plastic regime, the relation of the elastic-plastic regime given by

$$\frac{p_m}{s_Y} = 0.70 \ln\left(\frac{E^*d}{s_Y r'}\right) + 0.66, \qquad (1.78 \le E^*d / s_Y r' < 21), \qquad (13)$$

can be used to determine the interference distance for full plasticity. The representative strain, $E^*d / s_Y r'$, is also related to the normalized interference distance, *d/R*. By equating the mean contact pressure with the material hardness, the corresponding interference distance can be determined from the contact constitutive model (Eq. (13)). The number of independent variables can be reduced by using the hardness relation obtained from finite element simulations (Eq. (12)).

Because only shallow indentations are considered to obtain the minimum interference distance, the analysis can be simplified to that of a homogeneous half-space with layer material properties. Using Eqs. (12) and (13), the minimum interference distance is obtained as

$$\frac{d}{r'} = 1.41\left(\frac{s_Y}{E^*}\right)^{0.47} \qquad (14)$$

Hence, by introducing the indenter radius of curvature, the following relation must be satisfied in order for the real material hardness to be obtained,

$$\frac{d}{R}=\frac{2}{1+(r'/d)^2}\geq\frac{2}{1+0.50(E^*/s_Y)^{0.94}} \tag{15}$$

Equation (15) gives the minimum interference distance as a function of the indenter radius of curvature and effective elastic modulus-to-yield strength ratio . For relatively small values of E^*/s_Y (e.g., $E^*/s_Y = 10$), a deeper interference distance is needed for the mean contact pressure to reach a value equal to the material hardness (Fig. 2-4, Table 2). This is due to the increase of the material resistance to plastic flow with a decreasing E^*/s_Y. Equation (15) can be used to estimate the minimum interference distance if the elastic modulus and yield strength of the layer are known, and reflects the hardness dependence on geometry factors and material properties.

If the layer material properties are unknown, various indentation depths must be used to verify whether the minimum interference distance was reached. If the layer is too thin, there may be no indenter with sufficiently sharp tip to ensure that the minimum interference distance required to directly measure the layer hardness is less than the critical interference distance to avoid the substrate effect. In this case, the hardness of a very thin layer can be determined from the measured equivalent hardness using Eqs. (1) (or Eq. (8)) and (12).

From the variation of the hardness of the layered medium with the interference distance, it is possible to determine whether Eq. (1) or Eq. (8) describes the hardness of the layered medium. The compliance determined from the unloading portion of the indentation curve can be used to determine the value of $E_l/(1-n_l^2)$, because the effective elastic modulus of the layered medium is related to the initial unloading stiffness through $S \equiv dL/dd = 2rE_e^*$ (Sneddon, 1965), where the effective elastic modulus of a layered medium, E_e^*, is given by (King, 1987)

$$E_e^*=\left[\left(1-e^{-a h/r\sqrt{p}}\right)\frac{1-n_l^2}{E_l}+e^{-a h/r\sqrt{p}}\,\frac{1-n_s^2}{E_s}+\frac{1-n_i^2}{E_i}\right]^{-1}, \tag{16}$$

where a is a geometrical factor depending on the indenter shape, r is the radius of the projected contact area, and subscript i denotes the indenter material properties. However, the hardness of the layer cannot be calculated solely from either Eq. (1) or Eq. (8), because the yield strength of the layer is unknown, direct inversion of Eq. (1) or Eq. (8) is not possible. Therefore, Eq. (12) must be solved simultaneously with Eq. (1) or Eq. (8). According to Eq. (15), the interference distance must be greater than a minimum value that depends on the radius of curvature of the indenter tip and the layer material properties. Therefore, an arbitrary interference distance does not guarantee a valid hardness measurement. Instead, indentations for a series of interference distances must be performed in order to determine whether Eq. (1) or Eq. (8) should be used and to verify whether the real hardness of the layer was measured. Therefore, at each interference distance, Eqs. (1) (or Eq. (8)) and (12) are solved together, and the calculated hardness and yield strength of the layer, H_l^c and s_l^c, respectively, are obtained as functions of interference distance. (The term "calculated" is used to denote that the data do not necessarily correspond to the real layer material properties.) The calculated hardness (or mean contact pressure) increases with interference distance, reaching a peak value corresponding to the real material hardness, as shown in Fig. 2. If the calculated hardness versus interference distance curve increases continuously without reaching a maximum, then none of the data yields the material hardness. This would be the case of too shallow indentations, or too large radius of curvature of the indenter tip, to induce sufficient plasticity.

4. Numerical Simulation Results

Numerical results are presented in this section to demonstrate the appropriateness of the developed analysis for hardness measurement of layered media and to validate the hardness measurement scheme presented. For relatively hard layer of known thickness and unknown substrate material properties, the equivalent hardness of the layered medium can be assumed to be equal to the layer hardness, provided the interference distance is such that to avoid the substrate effect (Eq. (7)). As an example, consider a rigid spherical indenter and E_l = 168 GPa, s_l = 13 GPa, E_s = 130 GPa, s_s = 2.67 GPa, and $n_l = n_s$ = 0.3. Using Eq. (12), the layer hardness and the substrate hardness are found to be H_l = 24.5 GPa and H_s = 6.34 GPa, respectively. If the tolerance constant x is set equal to 10% and d/h is chosen to be 0.1, the equivalent hardness obtained from Eq. (1) is H_e = 23.2 GPa, which differs from the layer hardness by only 5%. Then, the minimum interference distance can be used either to verify whether the hardness of the layer was reached or to select the right indenter tip. Assuming a hard layer thickness equal to 100 nm, the interference distance for x = 0.1 is estimated to be less than 10 nm (Eq. (7)). To satisfy Eq. (15), $d/R \geq 0.28$; therefore, the indenter tip radius of curvature must be less than 35 nm.

A finite element simulation of a layered medium with a hard layer indented by a rigid sphere was performed to illustrate the hardness evaluation scheme presented in the previous section. The layer thickness and material properties used in this simulation were identical to those given in Table 1. It is assumed that these equivalent hardness data were obtained from an indentation test performed on a layer of given thickness and unknown material properties deposited on a substrate with known material properties. Figure 6 shows the indentation load, L, versus interference distance, d, of the layered medium obtained from the finite element analysis. The value of $E_l/(1-n_l^2)$, determined from the elastic stiffness (S = 2.94 μN/nm) obtained from the slope of the unloading curve at maximum load and Eq. (16), was found to be equal to 179 GPa, which differs from the input value in the finite element model by only 3%. Figure 7(a) shows finite element results for the equivalent hardness (or mean contact pressure) versus interference distance. Since the ratio between the equivalent hardness of the layered medium and the substrate hardness is greater than 1, it is concluded that the layer is harder than the substrate. In Eqs. (1) and (12) (using layer material properties) the values of H_e, $E_l/(1-n_l^2)$, $E_s/(1-n_s^2)$, s_s, d, and h are known. The value of H_s can be obtained from Eq. (12) using substrate material properties. Then, Eqs. (1) and (12) are solved simultaneously to obtain H_l^c and s_l^c at different interference distances using an iteration procedure. Results for the ratio of calculated and real layer properties are plotted in Fig. 7(b) in terms of interference distance. Both the calculated hardness and yield strength of the layer increase with interference distance, reaching a peak value at $d/R = 0.4$. According to the scheme proposed earlier, the calculated hardness and yield strength at $d/R = 0.4$ are the real material properties of the layer. Compared to the layer yield strength inputted in the finite element model and the hardness calculated from Eq. (12) using the material properties inputted in the finite element model, the error is less than 5%. For the layer material properties given in Table 1, Eq. (15) yields that the interference distance must be greater than 0.37R in order to obtain the real layer hardness, which is in fair agreement with the value predicted by the finite element simulation. Therefore, even for large plastic deformation and significant substrate effect, Eq. (15) can provide a fairly good estimate of the minimum interference distance required to obtain the real material hardness. Hence, this numerical experiment demonstrates the correctness of the proposed scheme.

The evolution of plasticity in the layer and substrate media of the previous simulation is shown in Fig. 8. At small interference distances (Figs. 8(a) and 8(b)) the plastic zone is confined in the layer and is similar to that obtained for a homogeneous medium (Figs. 3(a) and 3(b)). As the interference distance increases, plastic deformation initiates at the layer/substrate interface (Fig. 8(c)). Further penetration causes the plastic zone in the layer to grow toward the surface and the plastic zone in the substrate to expand downward and parallel to the interface (Figs. 8(d) and 8(e)). Eventually, the two plastic zones merge together (Fig. 8(f)). As can be seen in Fig. 8(f), the plastic zone in the substrate is comparable to that in the layer when $d/R = 0.4$, indicating that the substrate effect is significant.

5. Conclusions

A general hardness analysis for layered and homogeneous media was introduced that builds upon finite element simulation results and hardness relations derived in previous studies. In view of the presented results and discussion, the following main conclusion can be drawn.

(1) For the hardness of the layered medium to be close to that of the layer material, the interference distance must be less than a critical value that depends on the layer thickness and elastic-plastic properties of the layer and substrate materials in order to avoid the effects of the substrate deformation.

(2) For sufficient plasticity to occur in the layer such that the mean contact pressure to reach a value close to the real hardness of a material, the interference distance must be larger than a minimum value, which is a function of the radius of the indenter tip, effective elastic modulus, and yield strength of the material.

(3) The dependence of hardness on yield strength and elastic modulus was elucidated in light of finite element simulation results. A numerical scheme to determine the layer hardness from a series of indentation data was proposed and its effectiveness was validated by numerical results for a layered medium with a hard surface layer.

Acknowledgments

This research was partially supported by the National Storage Industry Consortium (NSIC), Extremely High Density Recording (EHDR) Program, and the Computer Mechanics Laboratory at the University of California at Berkeley.

References

Bhattacharya, A. K., and Nix, W. D., 1988, "Analysis of Elastic and Plastic Deformation Associated with Indentation Testing of Thin Films on Substrates," *International Journal of Solids and Structures*, **24**, pp. 1287-1298.

Chen, X., and Vlassak, J. J., 2001, "Numerical Study on the Measurement of Thin Film Mechanical Properties by Means of Nanoindentation," *Journal of Materials Research*, **16**, pp. 2974-2982.

Doerner, M. F., and Nix, W. D., 1986, "A Method for Interpreting the Data From Depth-Sensing Indention Instruments," *Journal of Materials Research*, **4**, pp. 601-609.

King, R. B., 1987, "Elastic Analysis of Some Punch Problems for a Layered Medium," *International Journal of Solids and Structures*, **23**, pp.1657-1664.

Komvopoulos, K., and Ye, N., 2001, "Three-Dimensional Contact Analysis of Elastic-Plastic Layered Media With Fractal Surface Topographies," *ASME Journal of Tribology*, **123**, pp. 632-640.

Lichinchi, M., Lenardi, C., Haupt, J., and Vitali, R., 1998, "Simulation of Berkovich nanoindentation experiments on thin films using finite element method," *Thin Solid Films*, **312**, pp. 240-248.

Loubet, J. L., Georges, J. M., Marchesini, O., and Meille, G., 1984 "Vickers Indentation Curves of Magnesium Oxide (MgO)**,"** *ASME Journal of Tribology*, **106**, pp. 43-48.

Marsh, D. M., 1964, "Plastic Flow in Glass," *Proceedings of the Royal Society* (London), Series A, **279**, pp. 420-435.

Martinez, E., and Esteve, J., 2001, "Nanoindentation Hardness Measurements Using Real-Shape

Indenters: Application to Extremely Hard and Elastic Materials," *Applied Physics A (Materials Science Processing)*, **A72**, pp. 319-324.

Mesarovic, S. Dj., and Fleck, N. A., 1999, "Spherical Indentation of Elastic-Plastic Solids," *Proceedings of the Royal Society* (London), Series A, **455**, pp. 2707-2728.

Oliver, W. C., and Pharr, G. M., 1992, "An Improved Technique for Determining Hardness and Elastic Modulus Using Load and Displacement Sensing Indentation Experiments," *Journal of Materials Research*, **7**, pp. 1564-1583.

Pelletier, H., Krier, J., Cornet, A., and Mille, P., 2000, "Limits of Using Bilinear Stress-Strain Curve for Finite Element Modeling of Nanoindentation Response on Bulk Materials," *Thin Solid Films*, **379**, pp. 147-155.

Pharr, G. M., 1998, "Measurement of mechanical properties by ultra-low load indentation," *Materials Science & Engineering A (Structural Materials: Properties, Microstructure and Processing)*, **A253**, pp. 151-159.

Sneddon, I. N., 1965, "The Relation Between Load and Penetration in the Axisymmetric Boussinesq Problem for a Punch of Arbitrary Profile," *International Journal of Engineering Science*, **3**, pp. 47-57.

Table 1. Thickness and properties of layer and substrate media of the finite element model

Medium	Layer	Substrate
Thickness, h/R	1	7
Elastic modulus, E (GPa)	168	160
Poisson ratio, n	0.3	0.3
Yield strength, s_l or s_s (GPa)	18.46	7

Table 2. Interference distance, equivalent strain, and mean contact pressure in Figs. 3 and 4.

E^*/s_Y	d/R	$E^* d/s_Y r'$	p_m/s_Y
10	0.072	1.93	1.12
	0.100	2.29	1.24
	0.200	3.33	1.50
	0.400	5.00	1.71
100	0.005	5.01	1.79
	0.007	5.93	1.91
	0.040	14.34	2.52
	0.059	17.48	2.58

List of Figures

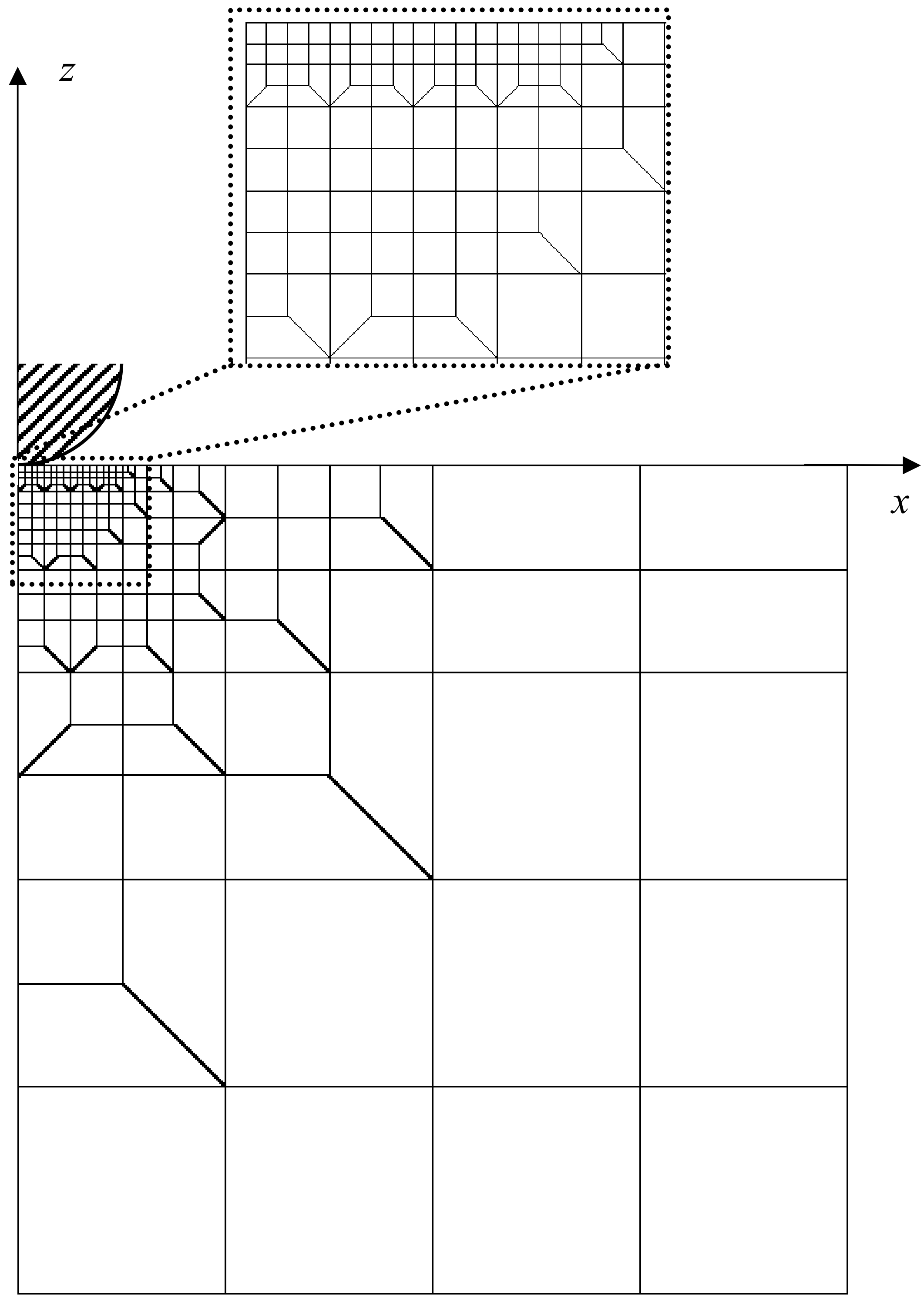

Figure 1

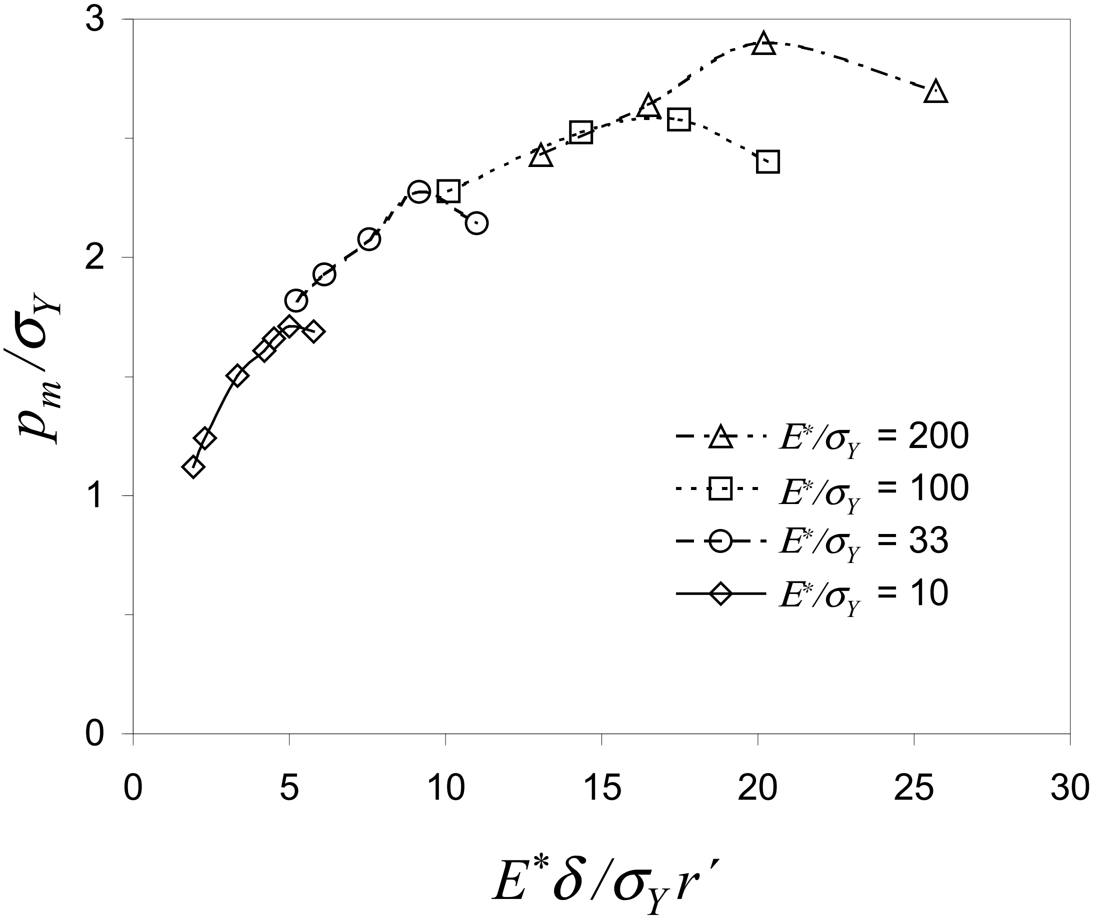

3
2
1
0
0
5
10
15
20
25
30
p_m/σ_Y
$E^*\delta/\sigma_Y r'$
E^*/σ_Y = 200
E^*/σ_Y = 100
E^*/σ_Y = 33
E^*/σ_Y = 10

Figure 2

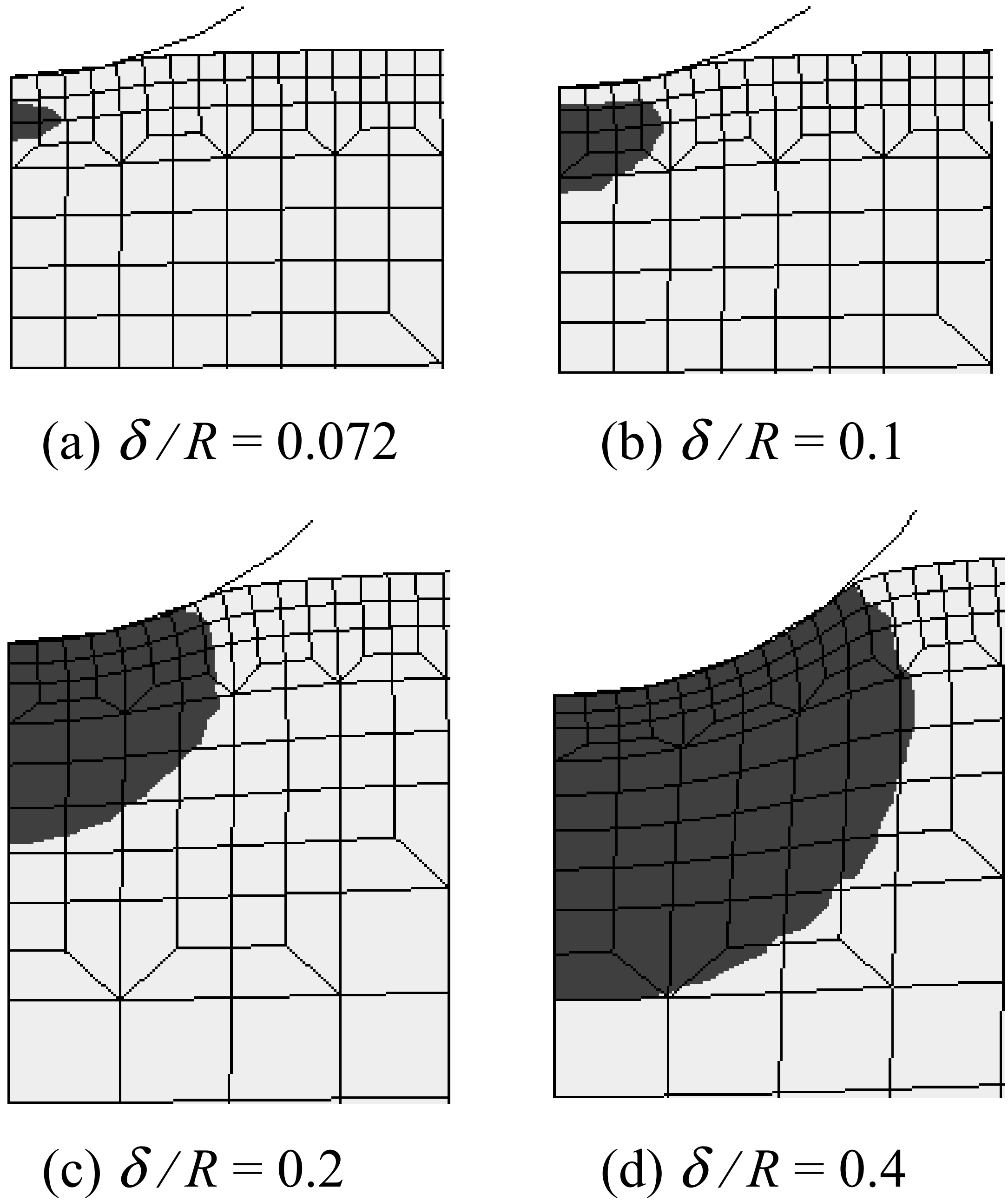

(a) $\delta / R = 0.072$ (b) $\delta / R = 0.1$

(c) $\delta / R = 0.2$ (d) $\delta / R = 0.4$

Figure 3

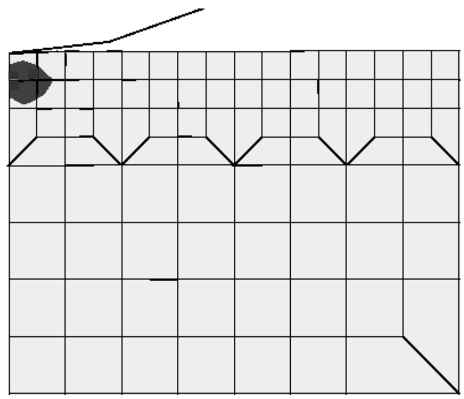

(a) $\delta / R = 0.005$

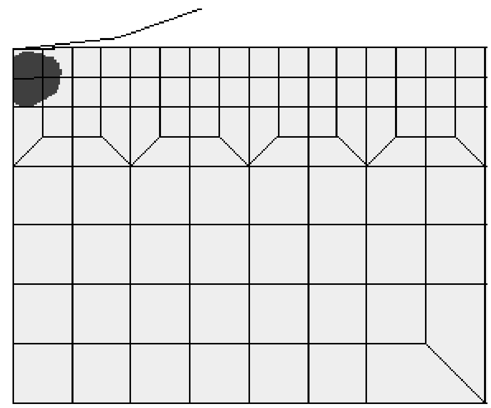

(b) $\delta / R = 0.007$

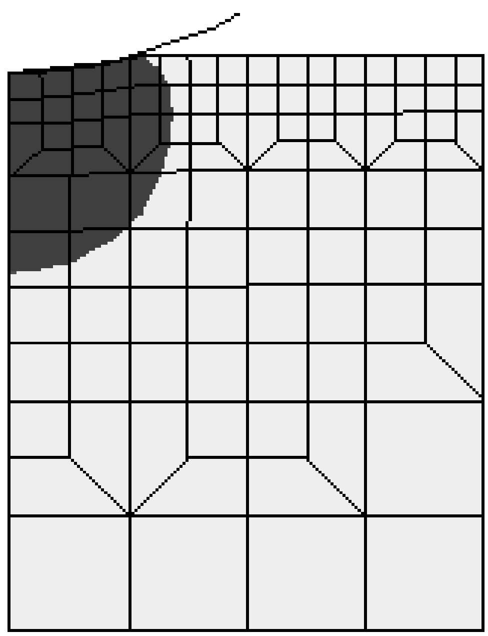

(c) $\delta / R = 0.04$

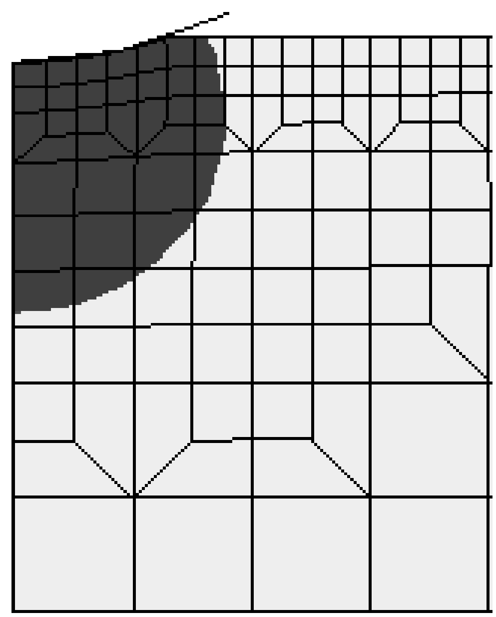

(d) $\delta / R = 0.059$

Figure 4

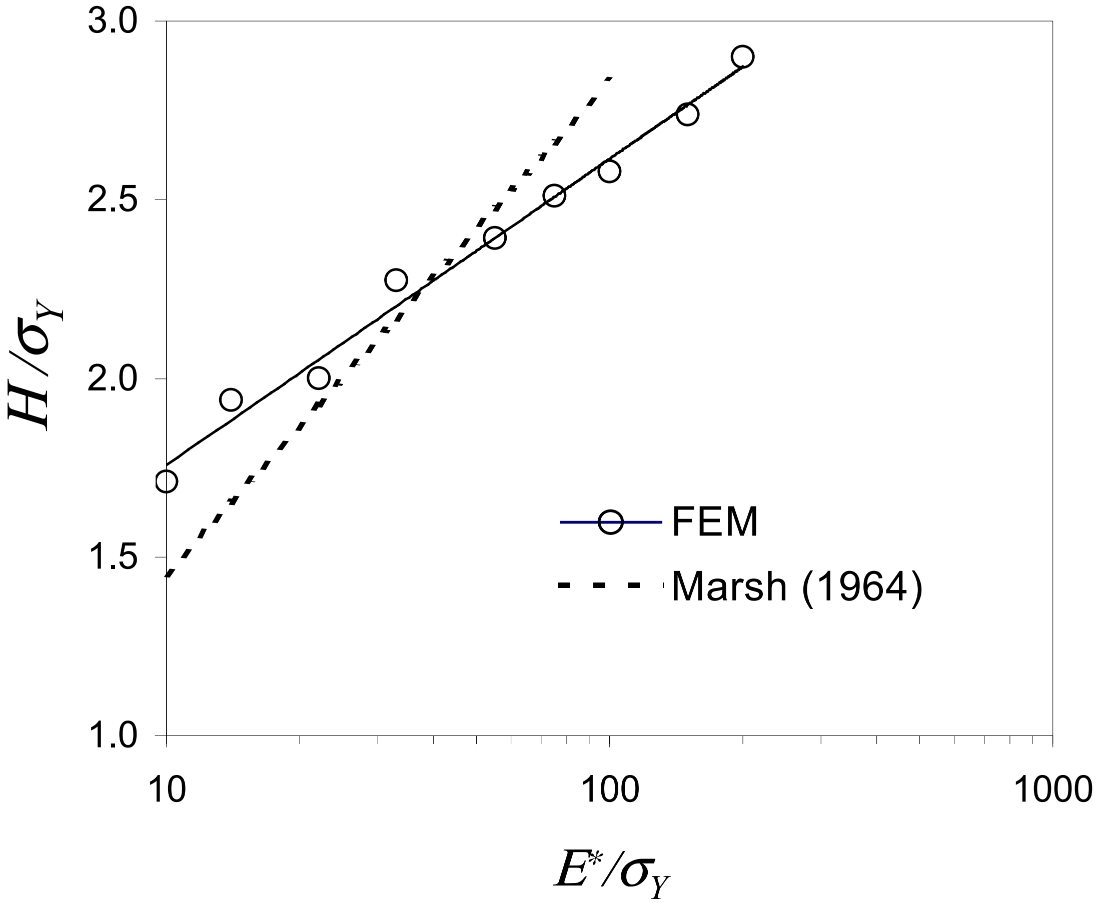

Figure 5

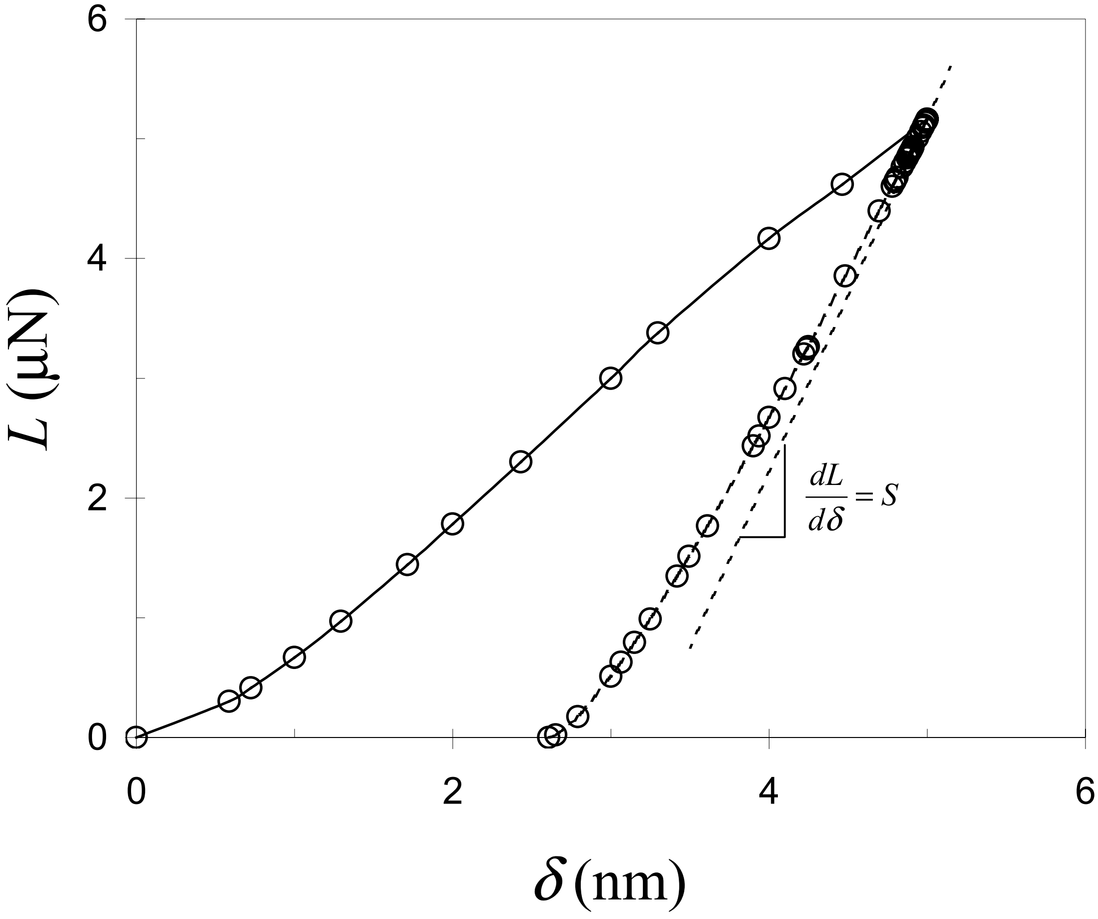

Figure 6

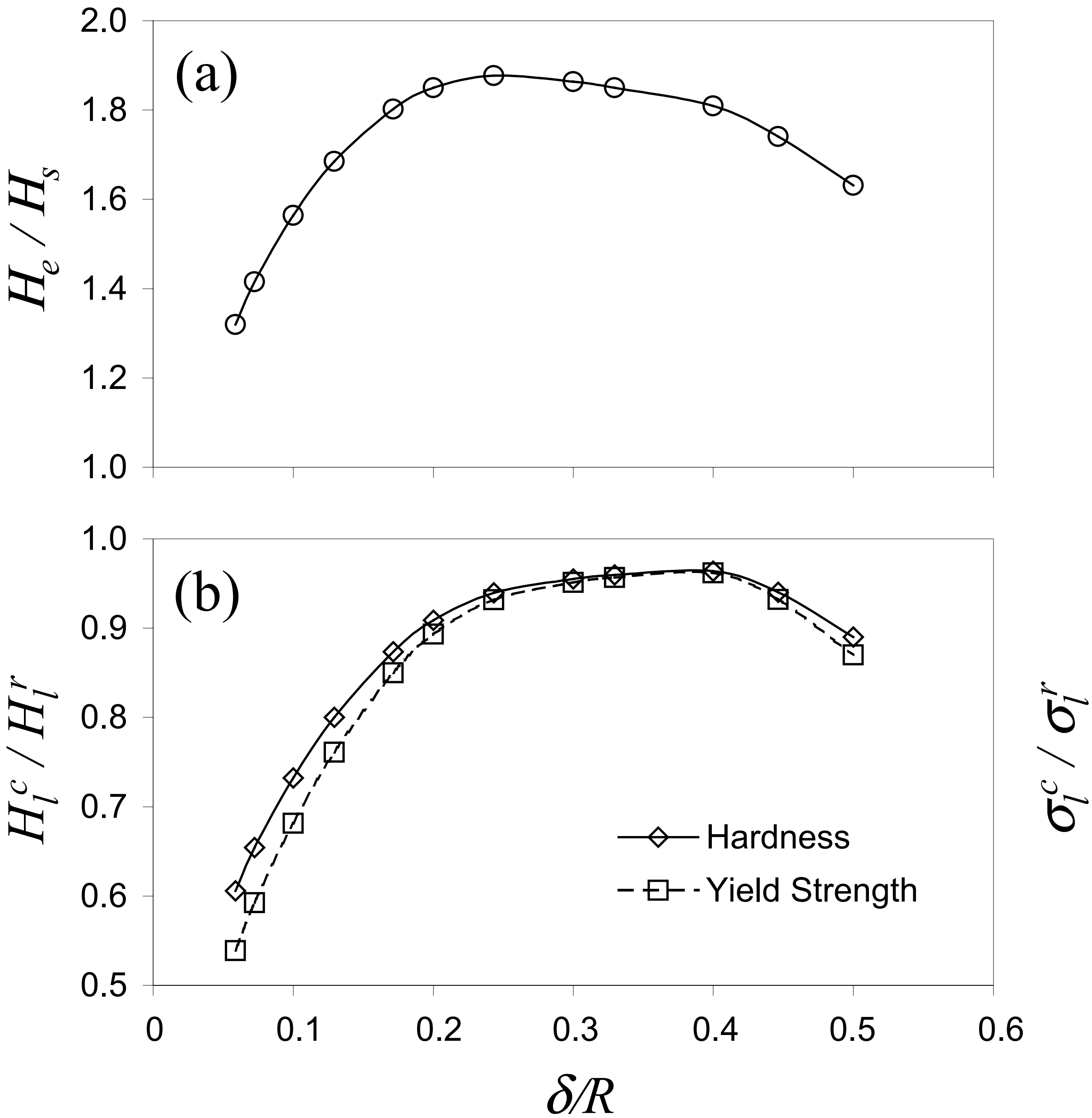
(a)
2.0
1.8
1.6
1.4
1.2
1.0
H_e / H_s
(b)
1.0
0.9
0.8
0.7
0.6
0.5
H_l^c / H_l^r
σ_l^c / σ_l^r
Hardness
Yield Strength
0
0.1
0.2
0.3
0.4
0.5
0.6
δ/R

Figure 7

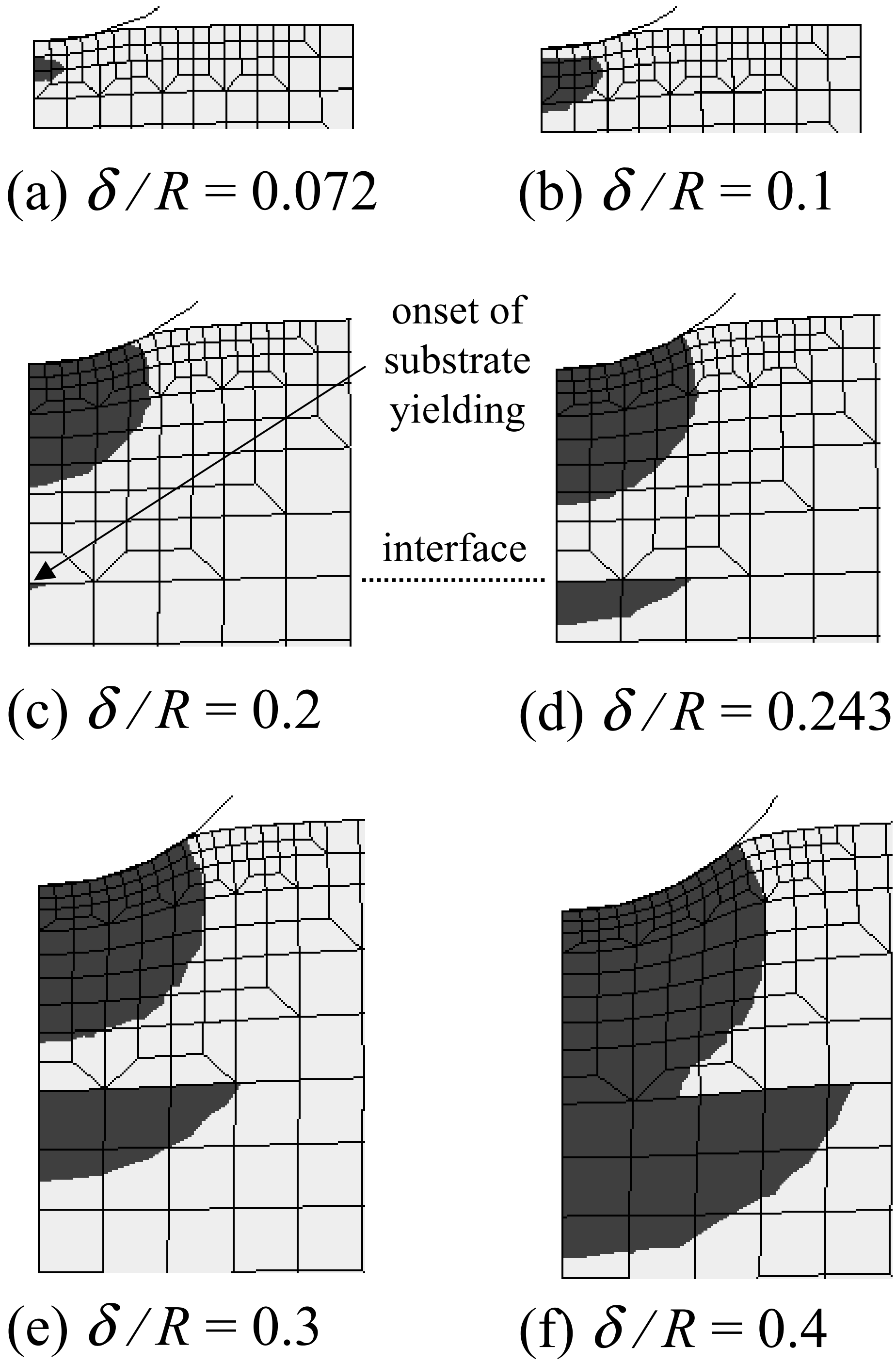
(a) $\delta / R = 0.072$
(b) $\delta / R = 0.1$
onset of
substrate
yielding
interface
(c) $\delta / R = 0.2$
(d) $\delta / R = 0.243$
(e) $\delta / R = 0.3$
(f) $\delta / R = 0.4$

Figure 8